## The impact of JPEG2000 lossy compression on the scientific quality of radio astronomy imagery

Sean M. Peters, Vyacheslav V. Kitaeff\*

International Centre for Radio Astronomy Research, The University of Western Australia, M468, 35 Stirling Hwy, Crawley 6009, WA, Australia

#### **Abstract**

The sheer volume of data anticipated to be captured by future radio telescopes, such as, The Square Kilometer Array (SKA) and its precursors present new data challenges, including the cost and technical feasibility of data transport and storage. Image and data compression are going to be important techniques to reduce the data size. We provide a quantitative analysis of the effects of JPEG2000's lossy wavelet image compression algorithm on the quality of the radio astronomy imagery data. This analysis is completed by evaluating the completeness, soundness and source parameterisation of the *Duchamp* source finder using compressed data. Here we found the JPEG2000 image compression has the potential to denoise image cubes, however this effect is only significant at high compression rates where the accuracy of source parameterisation is decreased.

The sheer volume of data anticipated to be captured by future resits precursors present new data challenges, including the cost at data compression are going to be important techniques to reduce of JPEG2000's lossy wavelet image compression algorithm on completed by evaluating the completeness, soundness and source data. Here we found the JPEG2000 image compression has the significant at high compression rates where the accuracy of source (ASKAP) telescope (DeBoer et al., 2009) is anticipated to capture spectral-imaging data-cubes (SIDCs) several orders of magnitude larger than any telescope ever before. The Square Kilometre Array (SKA) (Huynh and Lazio, 2013) SIDCs will be even larger, in the order of tens of terabytes per hour of observations. The networking, storing, processing and interrogating of such large datasets poses new technical, financial, and management challenges.

Such large SIDCs cannot be processed or stored on local user computers, even taking into account the projections for advances in HDD/SSD and network technologies, the cost of data storage will be significant. Any means to reduce the data volumes through compression will likely have significant benefits, especially in the reduction of the cost of the system.

Kitaeff et al. 2012 proposed the use of the JPEG2000 image standard as a method of storing SIDCs. JPEG2000 was first proposed in 1996 (Boliek, 1996) with remote sensing and medical imaging being the most demanding imaging fields in mind. The JPEG2000 group, established in 1999, has developed a standard containing 12 parts and defining the mechanisms not

The JPEG2000 group, established in 1999, has developed a standard containing 12 parts and defining the mechanisms not only for compression, but also for servicing and interrogating a broad range of imagery data<sup>1</sup>.

Kitaeff et al. 2014 details the relevant features and mechanics of JPEG2000.

The most distinctive difference between JPEG2000 and the original JPEG image standard is the use of the Discrete Wavelet Transform (DWT). The DWT is an algorithm to convert a signal to the time-frequency domain. Data in this domain lends itself particularly well to quantisation and compression (Taubman and Marcellin, 2002). As a result the JPEG2000 image standard can provide superior compression rates, with much less loss in visual quality, than any other standardised image format available. Additionally, JPEG2000 includes a variety of features especially useful for extremely large images such as: progressive transmission, the ability to decode any part of the image without having to decode the entire image, adaptive encoding with different fidelities through a precinct mechanism, multiple resolutions from a single master file. These features can significantly improve and enrich the interrogation of radio astronomy imagery data, as well as, reduce the overall volume of the data.

While JPEG2000 may retain visual content effectively at high compression rates, the effect of the lossy compression algorithm on the scientific quality of spectral image cubes captured in radio astronomy needs to be understood. One important way to study the impact of lossy compression on the quality of data is to see how well source finding algorithms identify the sources in compressed SIDCs.

While the volumes of data are large, the information density of the data is rather low. For example, for studies using HI emission of extragalactic objects, the majority of sources of such an emission will appear in data occupying only a few pixels. Such sources will be rather sparsely populating the volume of data-cube. The rest of imaging data is considered as noise.

<sup>\*</sup>Corresponding author

Email addresses: sean.peters.au@gmail.com (Sean M. Peters), slava.kitaeff@uwa.edu.au(Vyacheslav V. Kitaeff)

<sup>1</sup>http://www.jpeg.org/jpeg2000/

To distil the information from the volume of data it is therefore necessary to identify and parameterise the sources.

The development of fully automated source identification algorithms has recently become an intensive field of research (Whiting, 2012; Whiting and Humphreys, 2012; Floer and Winkel, 2012; Jurek, 2012; Boyce, 2003; Serra et al., 2012). These algorithms would normally construct a catalogue of sources from an astronomical image. Each entry in the constructed catalogue represents a source identified in the image, and its determined parameters. The unknown systematic errors introduced into the catalogue at any stage are of course very problematic. Thus, the source finding algorithms themselves need to be investigated, as well as, any additional data processing such as compression. The completeness and soundness are the main measures of how successful the algorithm is, in finding the sources (Popping et al., 2012). Such a set of metrics could be usefully utilised to study the impact of lossy compression on the quality of data, providing the guidance to the developers of the SKA as to whether JPEG2000's lossy compression may be safely used.

The rest of the paper is laid out as follows. Section 2 details the dataset used and methodology taken in conducting our experiment. Section 3 provides the results and detailed discussion on the experiments performed in this paper. Finally, we draw some conclusions in Section 4.

#### 2. Methodology

#### 2.1. Synthetic dataset

In order to test the impact of compression on the scientific quality of data, we have chosen to use a simulated SIDC in preference to real radio astronomy imagery. By using a simulated set of galaxies to create our imagery the true catalogue of sources within the image cube is known with a higher certainty. This helps with measuring, not only the accuracy of source identification after image compression, but source parameterisation as well. The Deep Investigations of Neutral Gas Origins (DINGO) (Meyer, 2009) synthetic SIDC was used in all our tests.

DINGO is one of the planned surveys to be performed by the ASKAP telescope. The synthetic SIDC was generated using an analytical galaxy simulation as described by Duffy et al. (2012), as part of survey planning. Significant effort was placed in creating a plausible DINGO survey simulation, as well as correctly inserting the sources while simulating instrumental noise and errors. A brief summary of the steps is outlined below:

- An analytical model for each of the different types of galaxies was produced. This was followed by a model of the distribution of these galaxies throughout the DINGO survey space.
- 2. A cosmological simulation was produced using the analytical models of galaxies and their distribution. This provided position, flux, HI content etc. for almost 4 million galaxies, the vast majority of which would be unidentifiable. These sources formed a true catalogue in our experiments. Many of the simulated sources, however, are too

faint to be observable with ASKAP. For the experiments performed in this paper a filter was applied on the true source catalogue (Duffy et al., 2012).

- 3. The galaxies were then injected into an empty image cube. At this point the dataset contains a perfectly clean set of galaxies distributed throughout the cube.
- Mock visibility data (radio telescopes capture data in the visibility domain - the Inverse Fourier Transform of the image cube) was then generated from the image cube using the *Miriad* software (Sault et al., 1995).
- The visibility data was then convolved with the dirty ASKAP beam, to introduce instrumental noise.
- The resultant visibility data was passed through the Fourier Transform and then convolved with the clean image cube.
- 7. Finally Gaussian noise was distributed over the entire image cube following the profile of thermal noise expected in the ASKAP telescope.

The entire datacube is approximately 1 Terabyte in size with dimensions  $3,600 \times 3,600 \times 23,060$ . The spatial region represented approximately  $60 \text{deg}^2$ . Each frequency channel in the cube (third dimension) has a width of 18.518 KHz.

Duchamp (Whiting, 2012) and several other used tools that were tested, required too much memory and computational power to feasibly process the entire cube at once, while meaningfully exploring the required parameter space of JPEG2000. Therefore extracts were taken from the original cube and each was tested independently.

The lower the frequency, the farther away the galaxies are in the cube due to the cosmological redshift of HI, and therefore the sources appear fainter towards the low frequency end of the cube. It was therefore important to test several subsets of data at different frequency ranges.

A subcube should also contain a sufficiently large number of sources in order to provide statistical significance in the tests. It was decided, arbitrarily, that the source finder should be able to identify at least 50 sources within the subcube.

At the low frequency end of DINGO datacube the signal-to-noise ratio for the sources becomes very small. It was established in tests that Duchamp was able to identify very few sources above the frequency plane  $\sim 15000$ , which was selected as a lower boundary for the frequency axes.

Table 1 shows the three subcubes extracted from DINGO cube to perform the tests. The Z references the frequency axes of the dataset. Larger Z corresponds to the lower frequency.

Table 2 shows the mean and variance of the datasets A, B and C.

Figures 1 and 2 depict a typical and corrupted by the instrumental effects frames of the used synthetic cube containing hundreds of point sources (dark pixels). For each of such sources HI spectral line profile exist in the Z dimension.

Dataset	$X_0$	<i>Y</i> <sub>0</sub>	$Z_0$	$\Delta X$	$\Delta Y$	$\Delta Z$
A	0	0	4000	3600	3600	100
В	0	0	7000	3600	3600	100
C	0	0	10100	3600	3600	100

Table 1: Subcubes selection within the DINGO datacube

Dataset	Mean	Variance (×10 <sup>-5</sup> )
A	$-8.534 \times 10^{-10}$	3.650
В	$9.588 \times 10^{-11}$	3.579
C	$6.252 \times 10^{-09}$	3.532

Table 2: Mean and Variance of each dataset.

#### 2.2. JPEG2000 encoding/decoding

Unlike the binary compression available through cfitsio or HDF5, JPEG2000 is a true image compression that takes advantage of the multidimensionality of data. Figure 3 depicts the stages of encoding in JPEG2000.

In the first stage, pre-processing is performed. Pre-processing actually contains three substages: Tiling, Level Offset, Reversible/Irreversible Color Transform. This stage pre-pares the data to correctly perform the Wavelet Transform. During the Wavelet Transform, image components are passed recursively through the low pass and high pass Wavelet filters. This enables an intra-component decorrelation that concentrates the image information in a small and very localised area. It enables the multi-resolution image representation. The result is that 4 sub-bands with the upper left one *LL* on Figure 3 containing all low frequencies (low resolution image), *HL* containing vertical high frequencies, LH containing horizontal high frequencies, and *HH* containing diagonal high frequencies. Successive decompositions are applied on the low frequencies *LL* recursively as many times as desired.

By itself the Wavelet Transform does not compress the image data; it restructures the image information so that it is easier to compress. Once the Discrete Wavelet Transform (DWT) has been applied, the output is quantified in Quantisation unit.

Before coding is performed, the sub-bands of each tile are further partitioned into small code-blocks (e.g. 64x64 or 32x32 samples) such that code blocks from a sub-band have the same size. Code-blocks are used to permit a flexible bit stream or-

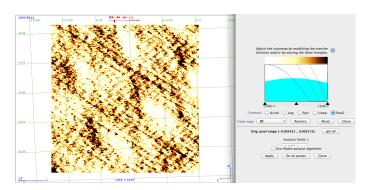


Figure 1: Typical single frequency frame of synthetic DINGO cube with a few hundred sources (darker pixels). The colours are artificial.

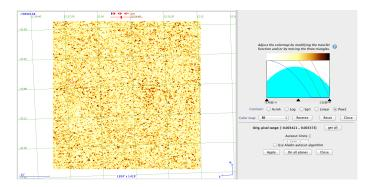


Figure 2: Corrupted by the instrumental effects single frequency frame of synthetic DINGO cube. The colours are artificial.

ganisation.

The quantised data is then encoded in the Entropy Coding unit. The Entropy Coding unit is composed of a Coefficient Bit Modeller and the Arithmetic Coder itself. The Arithmetic Coder removes the redundancy in the encoding of the data. It assigns short code-words to the more probable events and longer code-words to the less probable ones. The Bit Modeller estimates the probability of each possible event at each point in the coding stream.

At the same time as embedded block coding is being performed, the resulting bit streams for each code-block are organised into quality layers. A quality layer is a collection of some consecutive bit-plane coding passes from all code-blocks in all sub-bands and all components, or simply stated, from each tile. Each code-block can contribute an arbitrary number of bit-plane coding passes to a layer, but not all coding passes must be assigned to a quality layer. Every additional layer successively increases the image quality.

Once the image has been compressed, the compressed blocks are passed over to the Rate Control unit that determines the extent to which each block's embedded bit stream should be truncated in order to achieve the target bit rate. The ideal truncation strategy is one that minimises distortion while still reaching the target bit-rate.

In Data Ordering unit, the compressed data from the bit-plane coding passes are first separated into packets. One packet is generated for each precinct in a tile. A precinct is essentially a grouping of code blocks within a resolution level. Then, the packets are multiplexed together in an ordered manner to form one code-stream. There are five built-in ways to order the packets, called progressions, where position refers to the precinct number:

- Quality: layer, resolution, component, position
- Resolution 1: resolution, layer, component, position
- Resolution 2: resolution, position, component, layer
- Position: position, component, resolution, layer
- Component: component, position, resolution, layer

The decoder basically performs the opposite operations of the encoder.

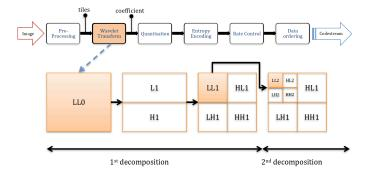


Figure 3: JPEG2000 encoding is based on discrete wavelet transformation, scalar quantisation, context modelling, arithmetic coding and post-compression rate allocation.

The details and mathematics of JPEG2000 encoding can be found in Gray 2003, Adams 2001, or Li 2003.

#### 2.3. Software

As JPEG2000 has not yet seen use in the radio astronomy domain many of the tools required, such as, source finders or image viewers did not provide direct support for the image standard. Several tools, therefore, were developed to support the experiments.

As the original dataset was stored using the HDF5 and FITS formats, we developed the *skuareview-encoder* and *skuareview-decoder* software<sup>2</sup>, to encode/decode the data to and from JPEG2000 using the JPEG2000 KDU library from Kakadu Software<sup>3</sup>.

The *Duchamp* source finder was used as the source identification software. *Duchamp* is the predecessor of the *Selavy* source finder (the source finder anticipated to be used in ASKAP and the SKA). Unfortunately *Selavy* was not made publicly available at the time of these works.

There are two particularly interesting aspects of *Duchamp* that are directly related to the experiments in this paper.

Firstly, *Duchamp* has the option to perform a wavelet reconstruction on the image cube before sources are searched for. This wavelet reconstruction aims to denoise the image. The "algorithme à trous" (Starck et al., 1994) is the wavelet transform used for this purpose as it maintains shift invariance where other wavelet transforms do not. The JPEG2000 image standard uses the Discrete Wavelet Transform (DWT) as a step in its compression algorithm. The DWT does not maintain shift invariance, however the algorithm is significantly less redundant as it includes subsampling (Bradley, 2003).

Secondly, *Duchamp* is known to be moderately inaccurate when parameterising sources found in the image (Westmeier et al., 2012). This must therefore be considered when measuring the accuracy of source parameterisation after JPEG2000 image compression.

#### 2.4. Experiment design

#### 2.4.1. Completeness and Soundness

The experiment aimed to provide a measure of the effect of the JPEG2000 image compression algorithm on the scientific quality of radio astronomy data. Here we define the scientific quality as the usefulness of the data to astrophysicists and their experiments. More specifically, we note that the only features important for DINGO science, found within a raw radio astronomy image cube are the HI sources within the cube; the vast majority of which represent the HI emission of distant galaxies. Everything else in the image cube is regarded as noise. As such, it is just the HI sources in the image that needed to be identified. This identification process needed to be as complete and as sound as possible, and each identified object needed to be parameterised as accurately as possible.

Source identification across an image cube is said to be complete if every source in the trueset catalogue is included in the identified set. The equation for completeness C is given by

$$C = \frac{P_{true}}{N} \tag{1}$$

where  $P_{true}$  represents all true positive identifications, and N is the number of sources in the trueset catalogue.

The source identification process is sound if every element in the identified set is included in the trueset catalogue. The equation for soundness S is given by

$$S = \frac{P_{true}}{P_{total}} \tag{2}$$

where  $P_{total}$  is the total number of detections that includes both, positive and negative detections.

To obtain the effect the JPEG2000 compression has on the completeness and soundness of the source finders we use measure "completeness difference"  $\psi$ , and "soundness difference"  $\omega$ . These measurements are defined by

$$\psi = C_{compressed} - C_{original} \tag{3}$$

$$\omega = S_{compressed} - S_{original} \tag{4}$$

where  $C_{compressed}$  and  $S_{compressed}$  are the completeness and soundness respectively calculated on the compressed dataset, and  $C_{original}$  and  $S_{original}$  are the completeness and soundness respectively calculated on the original dataset.

#### 2.4.2. Source Parameterisation

After identification, a source also needs to be parameterised. Each source is attributed to a location in galactic coordinates Right Ascension (RA), Declination (Dec) and Frequency. Beyond this a variety of parameters are used to specify the attributes of each source. In this test we investigated the parameters listed below:

- Right Ascension
- Declination
- Frequency

<sup>&</sup>lt;sup>2</sup>https://github.com/ICRAR/SkuareView

<sup>&</sup>lt;sup>3</sup>http://www.kakadusoftware.com/

- Right Ascension Width
- Declination Width
- Frequency Width
- Integrated Flux

We measured the difference in the performance of source parameterisation between the compressed dataset and the control dataset  $\gamma$ , for some JPEG2000 parameter k and some source parameter type p using the following equation

$$\gamma_k = \text{RMSE}_o(p) - \text{RMSE}_k(p) \tag{5}$$

where RMSE $_o$  is the Root Mean Square Error (RMSE) between the source parameter value identified with the original dataset, and the true source parameter, while RMSE $_k$  is the RMSE between the source parameter value identified with the dataset compressed with JPEG2000 parameter k, and the true source parameter value.

The value  $\gamma_k$  will thus be positive if the compressed dataset allows for more accurate parameterisation and negative otherwise.

For example, to measure the effect of JPEG2000's image compression algorithm on the parameterisation of sources with respect to the frequency width parameter of all sources identified, we calculate the RMSE of the frequency width of each source identified within the dataset by *Duchamp* against the trueset catalogue's frequency width for the respective parameter. We then perform the same RMSE calculation using the sources identified by *Duchamp* after compression. If the difference between the resultant RMSE from the compressed dataset, and the RMSE from the original dataset is positive, then the compressed dataset has allowed *Duchamp* to provide more accurate parameterisation. However, if this difference is negative this would imply the compression has damaged the scientific quality of the data.

#### 2.4.3. Cross matching

In order to correctly measure source parameterisation and the accuracy of the source finder, we need to ensure that the sources retrieved by the *Duchamp* are attributed to the correct source in the trueset catalogue.

This was done by iterating over all pairs  $(u_i, v_j)$  where  $u_i$  is the  $i^{th}$  source obtained from the *Duchamp* source finder and  $v_j$  is the  $j^{th}$  source from the true catalogue. A pair was considered a match if the following conditions were true:

#### 1. Condition 1

- (a) The center of  $u_i$  was contained within the bounds of  $v_i$ ,
- (b) **OR** the center of  $u_i$  was within 3 voxels of the center of  $v_j$ ,

#### 2. Condition 2

(a) if multiple sources from the *Duchamp* catalogue were potential matches with a single  $v_j$ , the  $u_i$  with the closest center to  $v_j$  was chosen.

# 2.4.4. Comparison of JPEG2000 against the Wavelet Reconstruction in Duchamp

This experiment was intended to evaluate the JPEG2000 lossy compression as a denoising tool, by drawing a comparison between JPEG2000 lossy compression and the wavelet reconstruction algorithm used in *Duchamp*.

The differences in completeness, soundness and source parameterisation were calculated between *Duchamp* with a wavelet reconstruction and *Duchamp* without the wavelet reconstruction. These results were then graphed alongside the differences in completeness, soundness and source parameterisation of *Duchamp* between compressed imagery and uncompressed imagery.

Only one set of parameters was used for the wavelet reconstruction as described in Table 3 due to the fact that as the *Duchamp* wavelet reconstruction was computationally exhaustive. These parameters were chosen with reference to experiments performed on similar datasets (Westmeier et al., 2012; Popping et al., 2012).

Parameter Name	Value	Comment	
minVoxels	7	Minimum voxels required to iden-	
		tify a source	
flagAdjacent	true	Identified objects are merged us-	
		ing adjacency	
snrCut	5	Threshold in multiples of stan-	
		dard deviation for the Isotropic	
		Undecimated Wavelet Transform	
		(IUWT) (Starck et al., 2007)	
scaleMin	2	Minimum wavelet scale in the	
		IUWT (Starck et al., 2007)	

Table 3: Duchamp source finder parameters

#### 2.4.5. JPEG2000 parameter space

In our experiment we selected four of the most important parameters to investigate from the JPEG2000 parameter space:

- The Quantisation step size is extremely influential on the compression ratio and lossiness of the JPEG2000 compression algorithm. Smaller step sizes will result in less quantisation and therefore less lossy compression. By exploring this parameter we can observe the influence of the JPEG2000 compression algorithm at different levels of lossiness.
- The number of *levels in the tree of the DWT* influences the structure of the wavelet domain before quantisation and compression.
- Precincts partition the image cube into rectangles that are each encoded independently. This will effect how the wavelet domain will be supplied to quantisation and compression resulting in differing compression ratios.
- The *Code block size* effects the size of the most granular partition in the JPEG2000 compression algorithm. Large

block sizes will provide more opportunity for compression.

These parameters were explored as described in Table 4.

Parameter Name	Default	Start	End	Step
Quantization step size	1/256	$10^{-6}$	0.01	×√√10
DWT levels	5	1	32	+4
Precincts	$2^{15}$	64	1024	×2
Code block size	64	4	64	×2

Table 4: JPEG2000 compression parameters iterated over in our experiment.

#### 2.4.6. Procedure

A script was developed in order to perform this experiment over multiple JPEG2000 parameters and multiple datasets. The process is described below using the following function definitions;

- Duchamp(D) takes dataset D and returns catalogue C.
- Process(C) takes catalogue C and retrieves the completeness, soundness and source parameterisation results R.
- Encode takes dataset D, parameter type j and parameter value i and returns the JPEG2000 lossily compressed image.
- Decode takes the JPEG2000 lossily compressed image and decodes it into a FITS (required by *Duchamp*) dataset.

```
\begin{split} &C_t \leftarrow \text{true catalogue} \\ &D_o \leftarrow \text{original dataset} \\ &C_o \leftarrow \text{Duchamp}(D_o) \\ &R_o \leftarrow \text{Process}(C_o) \\ &\textbf{for all JPEG2000 parameter types } j \text{ in Table 4 do} \\ &\textbf{for all values } i \text{ for parameter type } j \text{ in Table 4 do} \\ &D_j^i \leftarrow \text{Decode}(\text{Encode}(D_o, i, j)) \\ &\text{item } C_j^i \leftarrow \text{Duchamp}(D_j^i) \\ &\text{item } R_j^i \leftarrow \text{Process}(C_j^i) \\ &\textbf{end for} \\ &\textbf{for all } i \textbf{ do} \\ &\text{Graph}(R_j^i - R_o) \\ &\textbf{end for} \\ &\textbf{end for} \end{split}
```

3D WDT encoding may improve the efficiency of encoding (Delcourt et al., 2011), however, KDU library only enables 2D encoding with a possibility to use the image components as another dimension. Thus, in all of our tests frames of SIDC were encoded independently into the image components using 2D WDT.

#### 3. Results and Discussion

The presented results are based in intensive testing and many runs with different parameters. Due to the large data volumes many experiments require many hours to complete.

#### 3.1. Compression Ratio and RMSE

Fundamentally, our most important choice when using any lossy compression algorithm, is to what degree the data can be compressed without the introduction of a significant error. We explored a variety of parameters in our experiments and measured the effect of a change on each parameter on the scientific quality of our dataset. This effect on scientific quality can be more intuitively understood with reference to each parameter's effect on compression ratio and RMSE.

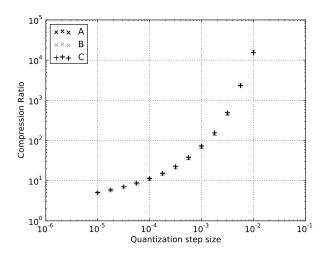


Figure 4: Compression Ratio vs Quantisation step size for datasets A, B and C.

Figure 4 demonstrates a direct exponential correlation between the quantization step size and the compression ratio of the JPEG2000 compression algorithm. This correlation was consistent across each dataset used. The quantization step size was observed over our results to be the most influential JPEG2000 parameter on the compression ratio and RMSE.

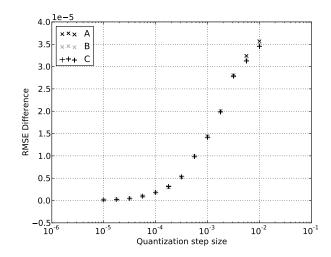


Figure 5: RMSE Difference vs Quantisation step size for datasets A, B and C.

As it can be expected, the RMSE Difference, which is a measure of difference of the original and compressed versions of

the image, is increasing with the quantisation step size (see Figure 5). This on its own does not indicate the ability of a source finder to detect the sources. In fact, the increasing RMSE difference of a noisy image (Fig.1) indicates a noise filtering effect produced by the compression. The question is how this impacts the sources in the image?

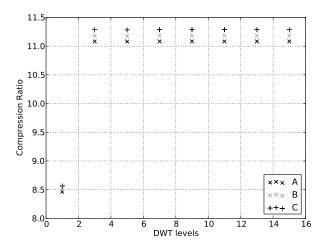


Figure 6: Compression Ratio vs DWT levels for datasets A, B and C.

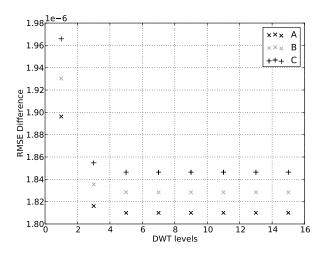


Figure 7: RMSE Difference vs DWT levels for datasets A, B and C.

Figures 6 and 7 show that the number of DWT levels did not significantly impact neither the compression ratio during the lossy compression or the RMSE difference, except for DWT=1.

#### 3.2. Completeness and Soundness

#### 3.2.1. Completeness

In Figure 8 it can be seen that in dataset A the source identification algorithm achieves equivalent completeness when compressed for almost all values of quantisation step size. There is a small dip just before an increase by as much as 3% in the completeness of the sources identified. This peak of completeness at a quantisation step size of  $3 \times 10^{-3}$  corresponds with an

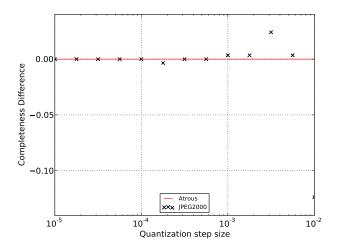


Figure 8: Completeness Difference vs Quantisation step size for dataset A.

extremely high compression ratio of over  $5 \times 10^2$ . The final data point captured shows a significant drop in completeness which simply corresponds to the image eventually losing all scientific quality at extremely high compression.

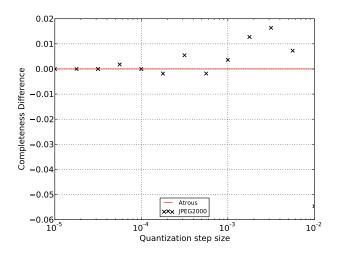


Figure 9: Completeness Difference vs Quantisation step size for dataset B.

Datasets B and C show similar results. In Figure 9 we observe that Duchamp achieves higher or equal completeness on a compressed dataset B for almost all data points. The completeness achieved in dataset B, was almost as high as 2%, occurring again at a high compression ratio of over  $4 \times 10^2$ .

Finally Figure 10 shows a steady increase in the completeness of *Duchamp* with respect to the quantisation step size in dataset *C*. Dataset *C* is particularly interesting as this dataset included, by far, the most sources. The vast majority of these sources are fainter and thus more difficult to observe. This experiment clearly shows the potential for JPEG2000 lossy compression to act as a denoising tool on spectral datasets to achieve higher completeness in source identification.

Figure 11 obtained on dataset A shows that the number of

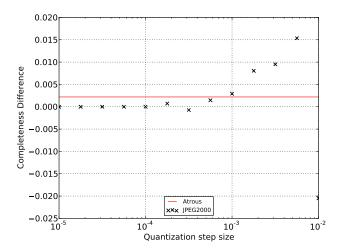


Figure 10: Completeness Difference vs Quantisation step size for dataset C.

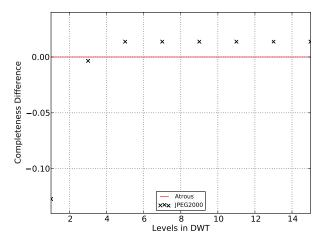


Figure 11: Completeness Difference vs DWT levels for dataset A.

DWT levels rather insignificantly influences the completeness of the source finding. Figure 12 depicting the completeness obtained in experiments with all datasets is also showing almost no effect of the number of DWT levels on the source finding. This means that most of the information about the sources are contained in the first few DWT levels, and further encoding is unnecessary.

The final two parameters, precinct size and block size, had no effect on the completeness or the soundness. This is somewhat expected as neither parameter has any direct effect on any of the lossy components within the JPEG2000 compression algorithm, rather they directly effect the lossless components e.g. run length encoding.

Figures 13, 14 and 15 show the completeness with respect to the integrated flux of a source for each dataset. The clear upward trend in all graphs is due to the fact that sources with higher total flux are easier identified. The dark 'x' data points correspond to the highest quantisation step size where the image is extremely compressed, resulting in significant loss in

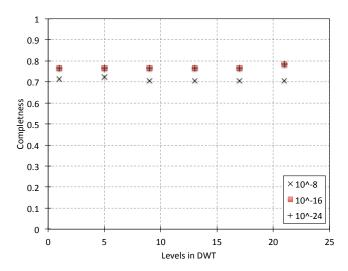


Figure 12: Completeness vs DWT levels for the quantisation step sizes  $10^{-8}$ ,  $10^{-16}$ ,  $10^{-24}$  for all datasets.

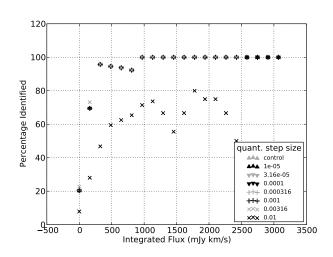


Figure 13: Completeness vs Integrated Flux for dataset *A* compressed with a variety of different quantisation step sizes. The points for all the used quantisation step sizes are superimposed, except for the step size 0.01.

completeness. Finally across all datasets it is apparent that more low integrated flux sources of less than 800 mJy per km/s are identified at higher quantisation step size compressions, which again lends to the conclusion that JPEG2000 has a denoising effect increasing the signal to noise ratio and allowing previously undetectable by the *Duchamp* sources to be identified.

In dataset A we found an improvement from the original completeness of 0.203 by  $\sim 3\%$  to 0.23, in dataset B the improvement increased the completeness from 0.089 to 0.11 and in dataset C the improvement had a peak increase of completeness from 0.028 to 0.043. This result conclusively shows JPEG2000 to be having a denoising effect on the simulated DINGO cube dataset.

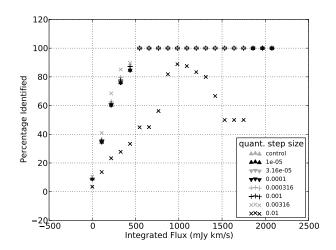


Figure 14: Completeness vs Integrated Flux for dataset B compressed with a variety of different quantization step sizes. The points for all the used quantisation step sizes are fully or partially superimposed, except for the step size 0.01

Dataset	Completeness	Soundness
A	0.203	0.766
В	0.089	0.576
C	0.028	0.704

Table 5: The completeness and soundness of Duchamp on the uncompressed datasets (Control).

### 3.2.2. Soundness

Completeness cannot be considered independently from the soundness of the source identification algorithms.

Figure 16 shows the comparison of the soundness on dataset A for the Duchamp's "algorithme à trous" (red line) and JPEG2000. One can see that the soundness remains fairly consistent for JPEG2000 until it drops off at the quantisation step approximately  $4 \times 10^{-2}$ . A small dip does exist in soundness at a quantization step size of approximately  $1 \times 10^{-3}$ . If we reference the respective completeness graph, Figure 8, we notice that the completeness appears to increase after this dip. This result is not unexpected as when the compression algorithm acts as a "filter" to the noise, the large structure instrumental noise will not be lost through the lossy compression. These stronger pieces of noise along with previously unidentified true sources are now more likely to be identified as a source. In fact with any source identification method that has a less than perfect soundness, if the completeness increases and the soundness remains stable both the true positives and false positives will increase. It is therefore quite probable that if just short of enough denoising is performed to identify a new true positive, there may be new false positives in our catalogue.

The soundness of *Duchamp* on dataset *B* and *C* stays the same or increases under JPEG2000 lossy compression for all data points excluding the final two as observed in Figures 17 and 18. In particular the soundness was only ever increased or exactly the same, at the average quantisation step size where completeness peaked. At high compression ratios JPEG2000 is

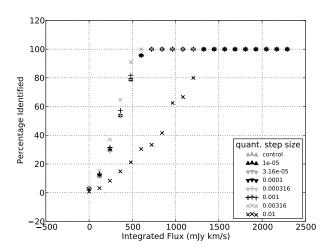


Figure 15: Completeness vs Integrated Flux for dataset C compressed with a variety of different quantisation step sizes. The points for all the used quantisation step sizes are fully or partially superimposed, except for the step size 0.01

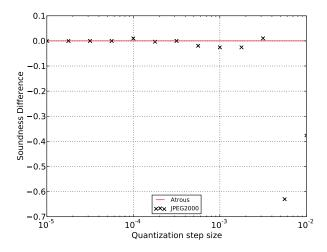


Figure 16: Soundness Difference vs Quantisation step size for dataset A.

known to occasionally cause ringing artefacts (Fang and Sun, 2007). If these ringing artefacts were to occur widely across the image the source finder may identify them as sources. This could potentially explain why we observe a loss in soundness at the highest compression ratios. We can note however, that this loss in soundness occurs after the average quantisation step size found to give peak completeness improvement to source identification. We therefore still find lossy JPEG2000 compression to improve completeness without loss in soundness at appropriate quantisation step sizes.

For all datasets however, the soundness fell dramatically for the final two quantisation step size. We can thus conclude that a quantisation step size of higher than  $6 \times 10^{-3}$  will negatively effect accurate source identification.

The number of DWT levels on the other hand, had a surprisingly negative correlation with the soundness of the *Duchamp* source finder as seen in Figure 19. It should, however, be noted

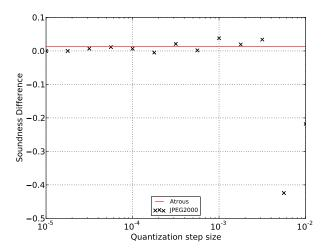


Figure 17: Soundness Difference vs Quantisation step size for dataset B.

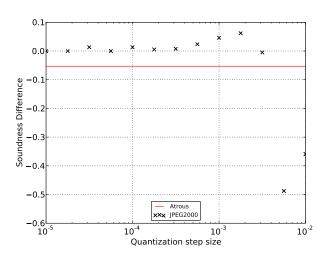


Figure 18: Soundness Difference vs Quantisation step size for dataset C.

that all data points in this Figure indicated the soundness to decrease after compression. As we have seen this is not the case, when exploring over the quantisation step size space, we can conclude that this is the result of high default quantisation step size of 1/256 used.

Overall we identify the quantisation step size to be the dominating parameter where a value of between  $1\times10^{-3}$  and  $3\times10^{-3}$  was found to be optimal to improve the completeness and soundness of source identification. Across all datasets the completeness and soundness trended upwards with respect to quantisation step size up to and including these data points. To optimise on particular datasets we would recommend searching between these values.

#### 3.2.3. The "algorithme à trous"

Overall the denoising effect of wavelet reconstruction in *Duchamp* was outperformed by the denoising effect of JPEG2000 image compression. In fact *Duchamp's* wavelet reconstruction had little effect at all on completeness and sound-

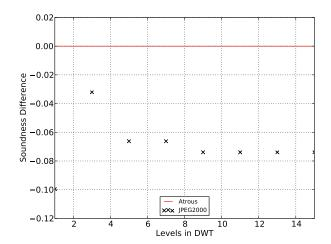


Figure 19: Soundness Difference vs DWT levels for dataset A.

Dataset	Duchamp with atrous	Duchamp with JP2
A	292min 32s	24min 12s
В	284min 16s	22min 43s
C	315min 11s	27min 6s

Table 6: The time taken for *Duchamp* with the wavelet reconstruction, versus time taken for *Duchamp* with encoding and decoding with JPEG2000

ness. As observed in Figure 18 dataset C was the only dataset to see an increase in source identification completeness after reconstruction, where that increase was only 0.25%. The soundness was positively effected in datasets B in Figure 17, but notably less so than the peak soundnesses found by simply compressing the image cube. Dataset A saw no effect on either soundness or completeness after a Duchamp wavelet reconstruction.

This lack of significant effect can be attributed to the parameter space of the wavelet reconstruction not being fully explored. It is also important to note that the *Duchamp* source finder's wavelet reconstruction has been improved in Duchamp's successor Selavy, to the reconstruction used by the 2D-1D wavelet reconstruction source identification algorithm (Floer and Winkel, 2012). The "algorithme à trous" found in *Duchamp* was also far more computationally expensive than the JPEG2000 compression algorithm. Table 6 shows for each dataset how much longer *Duchamp's* wavelet reconstruction took in comparison to how long encoding to JPEG2000, decoding back to FITS and then executing *Duchamp* without the wavelet reconstruction took.

It is, in fact, because of the computationally expensive nature of the wavelet reconstruction algorithm that a larger set of parameters could not be explored. Which lends to the hypothesis that the DWT in JPEG2000 as a denoising tool may be preferred over the "algorithme à trous" because while the DWT may include the undesirable trait of shift variance, the "algorithme à trous" is simply too slow for extremely large datasets. Furthermore, JPEG2000 can be used to generate compressed preview datasets for quality control and visual exploration of

data. Once generated with optimal parameters the previews can be used for source finding purposes removing a need for prior denoising, and substantially improving I/O performance due to the smaller size of compressed datasets.

#### 3.3. Source Parameterisation

#### 3.3.1. Right Ascension and Declination

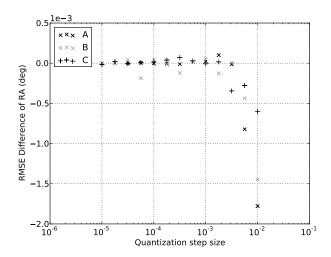


Figure 20: RMSE difference of RA vs Quantisation step size for all datasets.

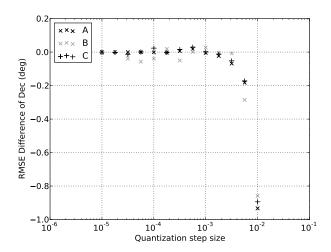


Figure 21: RMSE difference of Dec vs Quantisation step size for all datasets.

The spatial coordinates of sources identified by *Duchamp* appear to be more negatively affected by JPEG2000's lossy compression. We can observe in Figure 20 that when compressed with a quantisation step size of higher than approximately  $3 \times 10^{-4}$ , the accuracy of RA source parameterisation drops off. This is notably well before the quantisation step size resulting in a peak in completeness.

While the Dec source parameterisation in Figure 21 follows a similar trend, we identified what appeared to be an error in either the true-set catalogue's Dec parameter or *Duchamp's* Dec parameterisation. Sources that were identified with the exact

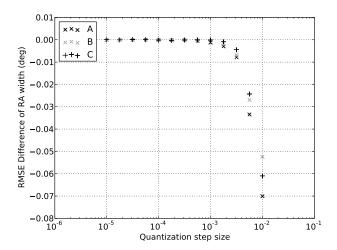


Figure 22: RMSE difference of RA width vs Quantisation step size for all datasets

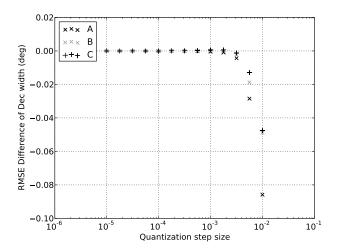


Figure 23: RMSE difference of Dec width vs Quantisation step size for all datasets.

same centroid voxel as found in the true catalogue were often found to have a Dec difference by as much as a degree. We can therefore not make any conclusive judgement from our results with regard to Dec source parameterisation.

Figures 22 and 23 both show a loss in the accuracy of spatial width parameterisation at high compression ratios. As the voxels become more correlated to each other through compression the soft edges of the sources appear to be either stretched above or below the threshold of a source. This directly shows that at high compression ratios of the JPEG2000 lossy compression algorithm, the scientific quality of radio astronomy data is negatively effected. At much more reasonable compression ratios, however, the effect is zero.

Overall source parameterisation of spatial width remained unaffected until compressed with a quantisation step size greater than  $1 \times 10^{-3}$  that corresponds to compression ratio approximately 1:100 (see Figure 4).

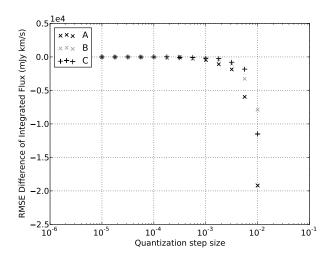


Figure 24: RMSE difference of Integrated Flux vs Quantisation step size for all datasets

#### 3.3.2. Integrated Flux

Figure 24 shows that across all datasets the parameterisation of integrated flux performs poorly at high compression rates (low quantisation step sizes). At high quantisation step sizes the domain of wavelet coefficients becomes more discretised. As these coefficients become more discretised the reconstruction will result in differing wavelet coefficient amplitudes. While the wavelet transform will still be capable of maintaining the structure of sources relative to the rest of the image, the original pixel amplitudes will change after reconstruction. Thus while the sources may still have amplitudes higher than neighbouring voxels, the actual value of the amplitude will have changed and while completeness can be increased, integrated flux source parameterisation is damaged.

In Section 3.2 it was identified that the peak completeness and soundness occurred between quantisation step sizes of  $1 \times 10^{-3}$  and  $3 \times 10^{-3}$ . We can clearly see in Figure 24 that by this point the source parameterisation of the source identification algorithm had been damaged.

We thus conclude, that in order to maintain as accurate as possible source parameterisation while using JPEG2000's lossy compression algorithm, one should not exceed the conservative limit of a compression ratio of 1:100 (or a quantisation step of approximately  $1 \times 10^{-3}$ ). Any kind of measurable negative impact on source parametrisation had not been observed at all on the compression ratios below 12, thus we can conclude that the compression did not affect the data in any negative way.

#### 4. Conclusion

JPEG2000 has been found to have a negligible effect on the scientific quality of radio astronomy imagery up to a compression ratio of approximately 12. Thereafter, source parameterisation would progressively become less accurate. At the same time, the completeness and soundness of source finding was increasing up to the compression ratios 1:100 and higher by as

much as 3% and 7% correspondently, as the result of noise filtering effect of the lossy wavelet JPEG2000 compression algorithm.

While the increase in completeness and soundness only occurred when source parameterisation had become less accurate, the result may still be useful. Further study is necessary to compare introduced errors due to the compression with other errors already present in the data. Such a study needs to be done with real rather than synthetic data.

JPEG2000 encoding had been found an order of magnitude faster than the "algorithme à trous" used by the Duchamp, and yet our results indicated the denoising effects of both to be comparable with JPEG2000 being slightly better. Future work should be placed into the investigation and implementation of a DWT based wavelet reconstruction, with quantisation and thresholding, to be used in source finders.

#### 5. Acknowledgements

A special thanks Prof. Amitava Datta for his guidance while preparing this work. Kakadu Software Ltd. and personally Prof. David Taubman for allowing us to freely use the software. Dr. Martin Meyer and Dr. Tobias Westmeier for their support in the use of the simulated DINGO cube dataset, and Dr. Attila Popping for other guidance in the Radio Astronomy domain.

#### References

Adams, M.D., 2001. The JPEG-2000 Still Image Compression Standard. Source 1. URL: http://www.jpeg.org/jpeg2000/wg1n2412.pdf.

Boliek, M., 1996. New work item proposal: JPEG2000 image coding system. Technical Report N390. ISO/IEC JTC1/SC29/WG1.

Boyce, P.J., 2003. Gamma Finder: a Java application to find galaxies in astronomical spectral line datacubes. M.sc. dissertation. School of Computer Science. Cardiff University.

Bradley, A., 2003. Shift-invariance in the discrete wavelet transform, in: DICTA, pp. 29–38. URL: http://www.cmis.csiro.au/Hugues. Talbot/dicta2003/cdrom/pdf/0029.pdf.

DeBoer D. et al., 2009. Australian ska pathfinder: A high-dynamic range widefield of view survey telescope. Proceedings of the IEEE 97, 1507–1521. doi:10.1109/JPROC.2009.2016516.

Delcourt, J., Mansouri, A., Sliwa, T., Voisin, Y., 2011. An evaluation framework and a benchmark for multi/hyperspectral image compression. Int. J. Comput. Vis. Image Process. 1, 55–71. URL: http://dx.doi.org/10.4018/ijcvip.2011010105, doi:10.4018/ijcvip.2011010105.

Duffy, A., Meyer, M., Staveley-Smith, L., Bernyk, M., Croton, D., Koribalski, B., Gerstmann, D., Westerlund, S., 2012. Predictions for askap neutral hydrogen surveys. Monthly Notices of the Royal Astronomical Society 426, 3385–3402.

Fang, J., Sun, J., 2007. Ringing artifact reduction for jpeg2000 images., in: ICIC (3), Springer. volume 2 of *Communications in Computer and Information Science*. pp. 1026–1034. URL: http://dblp.uni-trier.de/db/conf/icic/icic2007-3.html#FangS07.

Floer, L., Winkel, B., 2012. 2d-1d wavelet reconstruction as a tool for source finding in spectroscopic imaging surveys. Publications of the Astronomical Society of Australia 29, 244–250. URL: http://www.publish.csiro.au/paper/AS11042, doi:http://dx.doi.org/10.1071/AS11042.

Gray, K.L., 2003. The JPEG2000 Standard. Technical Report. Technische Universitat Munchen. URL: http://omen.cs.uni-magdeburg.de/itiamsl/cms/upload/lehre/winter04\_05/content.pdf.

Greisen, E., Calabretta, M., 2002. Representations of world coordinates in fits. Astron. Astrophys. 395, 1061–1075. URL: http://dx.doi.org/

- 10.1051/0004-6361:20021326, doi:10.1051/0004-6361:20021326, arXiv:astro-ph/0207407.
- Huynh, M., Lazio, J., 2013. An Overview of the Square Kilometre Array. ArXiv e-prints arXiv:1311.4288.
- Jurek, R., 2012. The characterised noise hi source finder: Detecting hi galaxies using a novel implementation of matched filtering. Publications of the Astronomical Society of Australia Publications of the Astronomical Society of Australia 29, 251–261. doi:10.1071/AS11044, arXiv:1112.1561.
- Kitaeff, V.V., Cannon, A., Peters, S.M., Wicenec, A., Taubman, D., 2014. The Future of Astronomical Data Formats III: Considerations For Contemporary Approach in Imagery. ArXiv e-prints arXiv:1403.2801.
- Kitaeff, V.V., Wu, C., Wicenec, A., Cannon, A.D., Vinsen, K., 2012. Skuare-view: Client-server framework for accessing extremely large radio astronomy image data., in: Proceedings of the 2012 Workshop on High-Performance Computing for Astronomy Date, ACM, New York, NY, USA. Astro-HPC '12. pp. 25–32. URL: http://doi.acm.org/10.1145/2286976.2286984, doi:10.1145/2286976.2286984.
- Li, J.I.N., 2003. Image Compression: The Mathematics of JPEG 2000. Signal Processing 46, 185–221.
- Meyer, M., 2009. Exploring the HI Universe with ASKAP, in: Panoramic Radio Astronomy: Wide-field 1-2 GHz Research on Galaxy Evolution. arXiv:0912.2167.
- Popping, A., Jurek, R., Westmeier, T., Serra, P., Floer, L., Meyer, M., Koribalski, B., 2012. Comparison of potential askap hi survey source finders. Publications of the Astronomical Society of Australia 29, 318–339. URL: http://journals.cambridge.org/article\_S132335800000134X, doi:10.1071/AS11067.
- Sault, J., Teuben, J., Wright, H., 1995. A retrospective view of MIRIAD, in: Astronomical Data Analysis Software and Systems IV, volume 77 of Astronomical Society of the Pacific Conference Series. pp. 433+. URL: http://adass.org/adass/proceedings/adass94/saultr.html.
- Serra, P., Jurek, R., Flöer, L., 2012. Using negative detections to estimate source-finder reliability. Publications of the Astronomical Society of Australia 29, 296–300. URL: http://journals.cambridge.org/article\_S1323358000001314, doi:10.1071/AS11065.
- Starck, J., Murtagh, F., Bijaoui, A., 1994. Image restoration with noise suppression using a wavelet transform and a multiresolution support constraint, in: Image Reconstruction and Restoration, SPIE. volume 2302. pp. 132–143. doi:10.1117/12.188035.
- Starck, J.L., Fadili, J., Murtagh, F., 2007. The undecimated wavelet decomposition and its reconstruction. IEEE Transactions on Image Processing 16, 297–309. doi:10.1109/TIP.2006.887733.
- Taubman, D.S., Marcellin, M.W., 2002. JPEG2000: Image Compression Fundamentals, Standards and Practice. Kluwer Academic Publishers, Boston.
- Westmeier, T., Popping, A., Serra, P., 2012. Basic testing of the duchamp source finder. Publications of the Astronomical Society of Australia 29, 276–295. URL: http://journals.cambridge.org/article\_S1323358000001302, doi:10.1071/AS11041.
- Whiting, M., Humphreys, B., 2012. Source-finding for the australian square kilometre array pathfinder. Publications of the Astronomical Society of Australia 29, 371–381. URL: http://journals.cambridge.org/article\_S1323358000001387, doi:10.1071/AS12028.
- Whiting, M.T., 2012. duchamp: a 3d source finder for spectral-line data. Monthly Notices of the Royal Astronomical Society 421, 3242–3256. URL: http://dx.doi.org/10.1111/j.1365-2966.2012.20548.x, doi:10.1111/j.1365-2966.2012.20548.x.